



Effect of lubricant temperature on the dynamic and stability behavior of journal bearing

Basim A. Abass, Zainab S. Hamzah

University of Babylon, College of Engineering, Department of Mechanical Engineering, Iraq.

Received 2 Jan. 2018; Received in revised form 20 Feb. 2018; Accepted 28 Feb. 2018; Available online 1 July 2018

Abstract

The effect of temperature on the dynamic behavior of journal bearing has been investigated in the present work. Time dependent Reynold's equation modified to include the effect of oil film temperature has been perturbed in order to calculate the eight dynamic coefficients required to evaluate the dynamic characteristics of the journal bearing. The oil film temperature was obtained by solving numerically the energy and heat conduction equation simultaneously with the Reynolds equation using appropriate boundary conditions. Suitable oil viscosity temperature has been used which couples the Reynolds and the energy equations. The effects of bearing aspect ratios and journal speed on the dynamic and stability characteristics of the rotor bearing system have been studied. Ranges of bearing aspect ratio from 0.5 to 1.5, speeds from 2000 to 8000 rpm have been considered. The mathematical model as well as the computer program prepared to solve the governing equations has been validated by comparing the results for the dynamic coefficients (stiffness and damping) obtained in the present work with that obtained experimental results from the literatures. The results seem to be in a good agreement with percentage of error less than 3%. Comparing to the isothermal analysis, a destabilizing effect has been noticed when the oil film temperature was considered. The results show that the critical mass decreases by 33% when the bearing works at an eccentricity ratio of 0.4.

Copyright © 2018 International Energy and Environment Foundation - All rights reserved.

Keywords: Journal bearing; Thermo-hydrodynamic; Reynolds equation; Dynamic coefficients; Perturbation technique; Stability.

1. Introduction

Relative rotational or linear movement between two parts can be ensured by widely used machine element called journal bearings. It consists of two surfaces in relative motion with thin film of viscous fluid between them which causes the hydrodynamic lubrication process. The dynamic as well as the static behavior of such bearings have been investigated by many workers. Lokhande and Prabhu [1] suggested method to include the variable viscosity of the oil in journal bearing by solving suitable energy equation which is uncoupled with the Reynold's equation. The static and the dynamic performances of the partial journal-bearing were considered. Pai and Majumdar [2] considered the thermal effect to investigate the stability of submerged oil journal bearings. Jakobson–Floberg- Olson model was used to investigate the cavitation region of the bearing. A peso-viscous oil model was taken into consideration by using the exponential law to describe the variation off the oil viscosity with the temperature. Paranjpe [3] used a transient thermo-

hydrodynamic to study the dynamically loaded engine bearings. Considerable variation in oil film temperatures has been noticed over time and space. The results obtained show that the adiabatic and simplified thermo-hydrodynamic analysis was well compared with the full thermo-hydrodynamic analysis. Significant improvement in the results has been obtained over the isothermal analysis. Michaud et al. [4] developed three dimensional transient thermo-hydrodynamic model to study the behavior of dynamically loaded journal bearing using finite element technique. Jacobson-Floberg-Olson model was used to predict the cavitation boundary. Bearings under sinusoidal loading have been studied using the proposed model. Paulsen et.al, [5] studied the journal bearing static and dynamic performance assuming both isothermal and thermal models. Stiffness, and damping coefficients as well as the load carrying capacity of the bearings are determined by the solution of the standard Reynolds and energy equations. The bearing performance was numerically investigated to study the effect of bearing geometry, rotational speed and the applied load. Rotor dynamics coupled with thermal effect for a continuous rotor shaft has been studied by Gu and Chu [6]. It was found that the analytical model can be used to evaluate different thermal vibration. Also it has been concluded that there are many factors affecting thermal vibration such as the shaft size, rotational speed, heating location and critical speed. Alves et al. [7] studied the dynamic behavior of the journal bearing regarding the threshold of instability. The dynamic of rotor has been discussed according to Lund critical mass and logarithmic decrement theories for thermo hydrodynamic model. It has been noticed that the oil viscosity is affected by the oil film temperature so that the bearing forces and dynamic stiffness and damping coefficients are modified. This means that the instability condition of the bearing is also modified. Hemmati et al. [8] developed dynamic analysis for short and long journal bearings working in laminar and turbulent regimes. Linear and non-linear stability of flexible rotor supported on short and long journal bearings were studied for both laminar and turbulent operating conditions. It was found that high static load can be used to eliminate the dangerous subcritical region for shafts supported on short journal bearings with shaft stiffness above critical value. The effect of axial groove at the inlet of oil film on the dynamic coefficients and linear stability has been discussed by Hamdavi et al. [9]. It has been noticed that one axial groove causes a remarkable deviation in the threshold speed values and frequency ratio. The present work aim to investigate the effect of induced oil film temperature on the dynamic coefficients and linear stability of the bearing since there is rare work related to this point.

2. Governing equations

In this work a finite length journal bearing is geometrically described in Figure 1 is considered. It consists of journal rotating around its center O_j with angular speed ω and fixed bearing with center O_b . Single axial groove of 20° width used to supply the lubricant inside the clearance gap of the bearing. The governing equations for the dynamic behavior of Nano lubricated journal bearing considering thermo-hydrodynamic analysis can be summarized as follow.

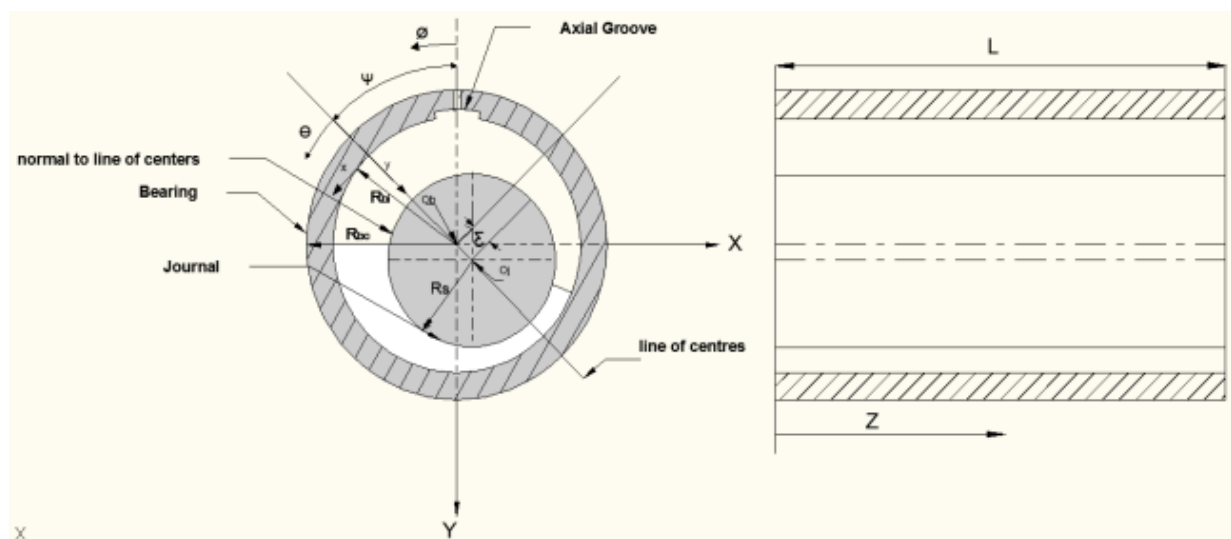


Figure 1. Journal bearing geometry.

3. Reynolds equation

The following modified time dependent Reynold's equation for Newtonian, laminar, peso-viscous flow was adopted [10].

$$\frac{\partial}{R \partial x} \left(G \frac{\partial P}{\partial x} \right) + \frac{\partial}{\partial z} \left(G \frac{\partial P}{\partial z} \right) = U \frac{\partial F}{R \partial x} + \frac{\partial h}{\partial t} \quad (1)$$

where:

$$G = \int_0^h \left[\frac{y}{\mu} \left(y - \frac{\int_0^h y/\mu \cdot dy}{\int_0^h 1/\mu \cdot dy} \right) \right] \cdot dy \quad (2)$$

$$F = 1 - \frac{\int_0^h y/\mu \cdot dy}{h \int_0^h 1/\mu \cdot dy} \quad (3)$$

The following non dimensional groups can be used to generalize equation (1).

$$\bar{P} = \frac{P c^2}{\mu_o \omega R_s R_{bi}}, \quad \bar{T} = \frac{T}{T_o}, \quad \bar{h} = \frac{h}{c}, \quad \bar{y} = \frac{y}{h}, \quad \theta = \frac{x}{R_{bi}}, \quad \bar{z} = \frac{z}{L}, \quad \bar{r} = \frac{r}{R_{bi}}, \quad \tau = \omega t, \quad \text{and } U = R\omega$$

Substituting the groups in equation (3.1) results in the following non-dimensional Reynold's equation:

$$\frac{\partial}{\partial \theta} \left(\bar{h}^3 \bar{G} \frac{\partial \bar{P}}{\partial \theta} \right) + \left(\frac{D}{2L} \right)^2 \frac{\partial}{\partial \bar{z}} \left(\bar{h}^3 \bar{G} \frac{\partial \bar{P}}{\partial \bar{z}} \right) = \frac{1}{2} \left(\frac{\partial \bar{F}}{\partial \theta} \right) + \frac{\partial \bar{h}}{\partial \tau} \quad (4)$$

where:

$$\bar{G} = \int_0^1 \left[\frac{\bar{y}}{\bar{\mu}} \left(y - \frac{\int_0^1 \bar{y}/\bar{\mu} \cdot d\bar{y}}{\int_0^1 1/\bar{\mu} \cdot d\bar{y}} \right) \right] \cdot d\bar{y} \quad (5)$$

$$\bar{F} = 1 - \frac{\int_0^1 \bar{y}/\bar{\mu} \cdot d\bar{y}}{\bar{h} \int_0^1 1/\bar{\mu} \cdot d\bar{y}} \quad (6)$$

The thickness of oil film for the aligned journal bearing can be expressed in dimensionless form as:

$$\bar{h} = 1 + \varepsilon \cos(\theta) \quad (7)$$

The Reynold's and energy equations are coupled by the viscosity of oil film, which was presupposed to be variables across the fluid film, in the axial, and around the circumference directions. The temperature of the oil viscosity dependence can be expressed as [11]:

$$\mu = \mu_o e^{-\beta(T-T_o)} \quad (8)$$

It can be expressed in non-dimensional form as: $\bar{\mu} = \frac{\mu}{\mu_o} = e^{-\beta T_o(\bar{T}-1)}$ where β is the thermo-viscous coefficient (1/°C). $\bar{T} = \frac{T}{T_o}$

4. Energy equation

The lubricant inside the clearance gap was sheared due to the shaft rotational speed and the oil viscosity causes a considerable shear stress. The energy equation governs the distribution of temperature in the oils film can be written in the dimensionless form [12].

$$P_e \left[\bar{u} \frac{\partial \bar{T}}{\partial \theta} + \left(\frac{\bar{v}}{c \cdot \bar{h}} - \bar{u} \frac{\partial \bar{h}}{\partial \theta} \right) \frac{\partial \bar{T}}{\partial \bar{y}} \right] = \frac{\partial^2 \bar{T}}{\bar{h}^2 \partial \bar{y}^2} + \frac{\bar{\mu}}{\bar{h}^2} N_d \left[\left(\frac{\partial \bar{u}}{\partial \bar{y}} \right)^2 + \left(\frac{\partial \bar{w}}{\partial \bar{y}} \right)^2 \right] \quad (9)$$

where u, v and w can be defined as [13]

$$\bar{u} = \frac{u}{U} = \bar{h}^2 \frac{\partial \bar{P}}{\partial \bar{\theta}} \left\{ \int_0^{\bar{y}} \frac{\bar{y}}{\bar{\mu}} d\bar{y} - \frac{\int_0^{\bar{y}} \frac{1}{\bar{\mu}} d\bar{y} \cdot \int_0^{\bar{y}} \frac{1}{\bar{\mu}} d\bar{y}}{\int_0^1 \frac{1}{\bar{\mu}} d\bar{y}} \right\} + \frac{\int_0^{\bar{y}} \frac{1}{\bar{\mu}} d\bar{y}}{\int_0^1 \frac{1}{\bar{\mu}} d\bar{y}} \quad (10)$$

$$\bar{v} = \frac{v}{U} \left(\frac{R_{bi}}{c} \right) = -\bar{h} \int_0^{\bar{y}} \left\{ \frac{\partial \bar{u}}{\partial \bar{\theta}} + \left(\frac{1}{2\gamma} \right) \frac{\partial \bar{w}}{\partial \bar{z}} - \frac{\bar{y}}{\bar{h}} \cdot \frac{\partial \bar{h}}{\partial \bar{\theta}} \frac{\partial \bar{u}}{\partial \bar{y}} \right\} d\bar{y} \quad (11)$$

$$\bar{w} = \frac{w}{U} = \bar{h}^2 \frac{\partial \bar{P}}{\partial \bar{z}} \left(\frac{1}{2\gamma} \right) \left\{ \int_0^{\bar{y}} \frac{\bar{y}}{\bar{\mu}} d\bar{y} - \frac{\int_0^{\bar{y}} \frac{1}{\bar{\mu}} d\bar{y} \cdot \int_0^{\bar{y}} \frac{1}{\bar{\mu}} d\bar{y}}{\int_0^1 \frac{1}{\bar{\mu}} d\bar{y}} \right\} \quad (12)$$

5. Heat conduction equation

The distribution of the temperature through a bearing (bush) can be estimated by solving the following equation for heat conduction through solids which can be written in the dimensionless form as [12].

$$\frac{\partial^2 \bar{T}_b}{\partial \bar{r}^2} + \frac{1}{\bar{r}} \frac{\partial \bar{T}_b}{\partial \bar{r}} + \frac{1}{\bar{r}^2} \frac{\partial^2 \bar{T}_b}{\partial \bar{\theta}} \quad (13)$$

6. Dynamic coefficients

The dynamic coefficients required to analyze the dynamic behavior can be evaluated by calculating the bearing load components and finding the bearing parameters at the equilibrium position of the journal center. For this purpose the modified Reynolds equation (4) has been using suitable perturbation technique. The approach proposed by Weimin et al. [14], Roy and Kakoty [15], and finally followed by Abass and Munier [16] was adopted to perturb such equation. This approach depends on the following assumptions for the bearing eccentricity ratio, attitude angle and oil film pressure. The eccentricity ratio and attitude angle can be perturbed as follows:

$$\varepsilon = \varepsilon_0 + E_0 e^{i\Omega t} \quad (14)$$

$$\psi = \psi_0 + \Psi_0 e^{i\Omega t} \quad (15)$$

By substitute equations (14) and (15) into equation (7) the following equation perturbed equation for the oil film thickness can be obtained:

$$\bar{h} = \bar{h}_0 + \bar{h}_1 e^{i\Omega \tau} = \bar{h}_0 + (E_0 \cos \theta + \varepsilon_0 \Psi_0 \sin \theta) e^{i\Omega \tau} \quad (16)$$

The hydrodynamic pressure can be perturbed and expressed as [14]:

$$\bar{P} = \bar{P}_0 + \bar{Q}_{10} e^{i\Omega \tau} + \bar{Q}_{20} e^{2i\Omega \tau} + \dots \quad (17)$$

By Substituting equations (16) and (17) into equation (1) and collecting the terms the following equations for pressures type zero, one and two (\bar{P}_0 , \bar{P}_1 and \bar{P}_2) can be obtained:

$$\frac{\partial}{\partial \theta} \left(\bar{h}_0^3 \bar{G} \frac{\partial \bar{P}_0}{\partial \theta} \right) + \left(\frac{D}{2L} \right)^2 \frac{\partial}{\partial \bar{z}} \left(\bar{h}_0^3 \bar{G} \frac{\partial \bar{P}_0}{\partial \bar{z}} \right) = \left(\frac{\partial \bar{F} \bar{h}_0}{\partial \theta} \right) \quad (18)$$

$$\frac{\partial}{\partial \theta} \left(\bar{h}_0^3 \bar{G} \frac{\partial \bar{P}_1}{\partial \theta} \right) + \left(\frac{D}{2L} \right)^2 \frac{\partial}{\partial \bar{z}} \left(\bar{h}_0^3 \bar{G} \frac{\partial \bar{P}_1}{\partial \bar{z}} \right) + \frac{\partial}{\partial \theta} \left(3\bar{h}_0^2 \cos \theta \bar{G} \frac{\partial \bar{P}_0}{\partial \theta} \right) + \left(\frac{D}{2L} \right)^2 \frac{\partial}{\partial \bar{z}} \left(3\bar{h}_0^2 \cos \theta \bar{G} \frac{\partial \bar{P}_0}{\partial \bar{z}} \right) = \left(\frac{\partial \bar{F} \cos \theta}{\partial \theta} \right) + i\Omega \cos \theta \quad (19)$$

$$\frac{\partial}{\partial \theta} \left(\bar{h}_0^3 \bar{G} \frac{\partial \bar{P}_2}{\partial \theta} \right) + \left(\frac{D}{2L} \right)^2 \frac{\partial}{\partial \bar{z}} \left(\bar{h}_0^3 \bar{G} \frac{\partial \bar{P}_2}{\partial \bar{z}} \right) + \frac{\partial}{\partial \theta} \left(3\bar{h}_0^2 \sin \theta \bar{G} \frac{\partial \bar{P}_0}{\partial \theta} \right) + \left(\frac{D}{2L} \right)^2 \frac{\partial}{\partial \bar{z}} \left(3\bar{h}_0^2 \sin \theta \bar{G} \frac{\partial \bar{P}_0}{\partial \bar{z}} \right) = \left(\frac{\partial \bar{F} \sin \theta}{\partial \theta} \right) + i\Omega \sin \theta \quad (20)$$

It is clear that equation (18) is just the steady state Reynolds equation of the journal bearing. It can be used to evaluate the bearing parameters at the equilibrium position of the journal center. The following Reynolds boundary conditions can be used to solve the Reynolds equation.

$$\bar{P}_0 = \frac{\partial \bar{P}_0}{\partial \theta} = 0 \quad \text{at} \quad \theta = \theta_c$$

The finite difference technique (iterative procedure with successive over relaxation) has been used to solve equation (18). The load components can be calculated as:

$$\bar{F}_{x_0} = - \int_0^1 \int_0^{2\pi} \bar{P}_0 \cos \theta \, d\theta \, d\bar{z} \quad (21)$$

$$\bar{F}_{y_0} = - \int_0^1 \int_0^{2\pi} \bar{P}_0 \sin \theta \, d\theta \, d\bar{z} \quad (22)$$

The oil film temperature affect the equilibrium position of the journal center which is known as the point at which the vertical hydrodynamic force component equal to the external applied load. The key in calculating the dynamic coefficients is the calculation of the equilibrium position. When the journal center forced to move out of its equilibrium position two additional disturbance pressures P_1 and P_2 is introduced. The linear stiffness coefficients can be found by integrating the linear pressure over the bearing surface as below, [17].

$$\bar{F}_{x1} = \int_0^1 \int_0^{2\pi} \bar{P}_1 \cos \theta \, d\theta \, d\bar{z} \quad \bar{F}_{y1} = \int_0^1 \int_0^{2\pi} \bar{P}_1 \sin \theta \, d\theta \, d\bar{z} \quad (23)$$

$$\bar{F}_{x2} = \int_0^1 \int_0^{2\pi} \bar{P}_2 \cos \theta \, d\theta \, d\bar{z} \quad \bar{F}_{y2} = \int_0^1 \int_0^{2\pi} \bar{P}_2 \sin \theta \, d\theta \, d\bar{z} \quad (24)$$

The dynamic coefficients can be expressed as: $K_{xx} = \frac{\partial F_x}{\partial x}$, $K_{xy} = \frac{\partial F_x}{\partial y}$, $K_{yx} = \frac{\partial F_y}{\partial x}$, $K_{yy} = \frac{\partial F_y}{\partial y}$, $C_{xx} = \frac{\partial F_x}{\partial \dot{x}}$, $C_{xy} = \frac{\partial F_x}{\partial \dot{y}}$, $C_{yx} = \frac{\partial F_y}{\partial \dot{x}}$, $C_{yy} = \frac{\partial F_y}{\partial \dot{y}}$. The linear dynamic coefficients can be expressed as:

$$\begin{aligned} \bar{K}_{xx} &= -\text{Re}(\bar{F}_{x1}) & \bar{K}_{yx} &= -\text{Re}(\bar{F}_{y1}) \\ \bar{K}_{xy} &= -\text{Re}(\bar{F}_{x2}) & \bar{K}_{yy} &= -\text{Re}(\bar{F}_{y2}) \\ \bar{C}_{xx} &= -\text{Im}(\bar{F}_{x1}) & \bar{C}_{yx} &= -\text{Im}(\bar{F}_{y1}) \\ \bar{C}_{xy} &= -\text{Im}(\bar{F}_{x2}) & \bar{C}_{yy} &= -\text{Im}(\bar{F}_{y2}) \end{aligned} \quad (25)$$

The obtained dynamic coefficients are substituted in the equations of motion for the standard Jeffcott model with rigid rotor as in [17] so that the equivalent stiffness coefficient K_{eq} , and the whirl frequency ω_n can be calculated from as

$$K_{eq} = \frac{(K_{xx} * C_{yy}) + (K_{yy} * C_{xx}) - (K_{xy} * C_{yx}) - (K_{yx} * C_{xy})}{(C_{xx} + C_{yy})} \quad (26)$$

$$\omega_n^2 = \frac{(K_{eq} - K_{xx}) + (K_{eq} - K_{yy}) - (K_{xy} * K_{yx})}{(C_{xx} * C_{yy}) - (C_{xy} * C_{yx})} \quad (27)$$

Also, can be evaluated the critical mass parameter from the below expression:

$$M = \frac{K_{eq}}{\omega_n^2} \quad (28)$$

7. Results and discussion

The results presented are obtained for the bearing with the working parameters shown in Table 1. The mathematical model and the computer program prepared to solve the governing equations used in this study have been verified by comparing the results for the different dynamic coefficients (stiffness and damping) obtained with that obtained by Sheeja and Prabhu [18] as presented in Figure 2. Both the stiffness and the damping coefficients have been drawn against the eccentricity ratio. It clearly depicts from this figure that the results are in a good agreement with percentage deviation less than 3%.

The dynamic coefficients (stiffness and damping) are studied for bearings with various L/D ratios (0.5, 1.0 and 1.5). The effect of this parameter on stiffness coefficients for a single grooved journal bearing considering thermal effect can be shown in Figures 3a to 3d. The non-dimensional bearing stiffness coefficients have been presented against the bearing eccentricity ratio. The presentation of direct stiffness coefficient (K_{xx}) obtained in the present study against the bearing eccentricity ratios shows that this coefficient in general increases for the bearing with higher eccentricity ratio as presented in Figure 3a. This can be imputed to the increase in load component in x-direction. Also this figure clearly shows that the

stiffness coefficient (K_{xx}) decreases for the bearings with higher aspect ratio which refers to the lower value of the force component in the x-direction. The percentage decrease in (K_{xx}) coefficient has been calculated for a bearing working at an eccentricity ratio ($\varepsilon = 0.6$) and it was found to be (11%, 29%) for the bearing that has aspect ratio of 1 and 1.5 in comparison with that of $L/D=0.5$. The similar above discussion can be re-confirmed to the cross coupled stiffness coefficient (K_{xy}). It can be shown from Figure 3b, the cross-coupled stiffness (K_{yx}) shows negative values as can be seen from Figure 3c. It was noticed that (K_{yx}) is slightly increases with the increase of (L/D) ratios when the bearing works at eccentricity ratios less than (0.6) after that the effect of the bearing aspect ratio becomes negligible. Figure 3d presents that (K_{yy}) decreases with the increase of (L/D) ratios. This figure also depicts that (K_{yy}) increases when the bearing works at higher eccentricity ratios. This can be imputed to the effect of the oil viscosity temperature relation.

Table 1. Geometric and operation parameters of the journal bearing [12].

Parameter	Symbol	Value and units
Bearing length	L	0.08 m
External bearing radius	R_{bout}	0.01 m
Shaft radius	R_s	0.05 m
Radial clearance	c	0.0000152 m
Inlet oil temperature	T_{in}	40°C
Inlet lubricant pressure	P_{in}	70000 Pa
Rotational speed	N	2000-8000 rpm
Oil density	ρ	860 kg/m ³
Inlet oil viscosity	μ_o	0.0277Pa.s
thermo-viscosity parameter	β	0.034
oil specific heat	C_o	2000 J/kg. °C
Oil thermal conductivity	K_f	0.13 W/m . °C
Bush thermal conductivity	K_b	250 W/m . °C
Bush convection heat transfer coefficient	h_{conv}	80 W/m ² . °C
Groove angle	θ_g	18 deg

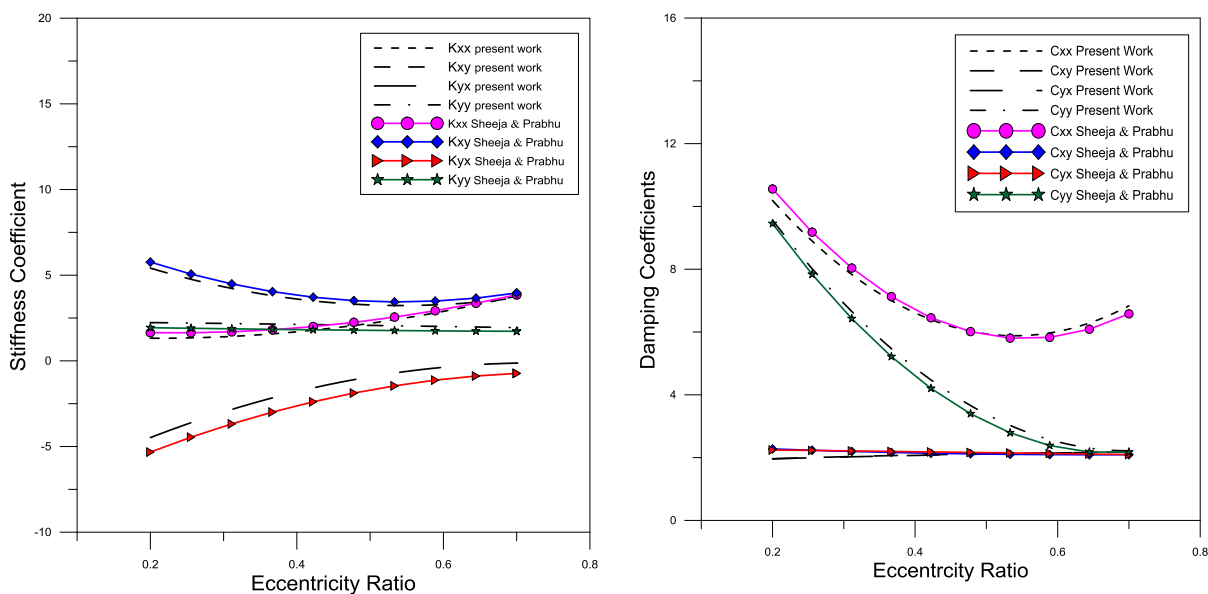


Figure 2. Comparison between the dynamic coefficients obtained in the present work and that obtained in ref. [18].

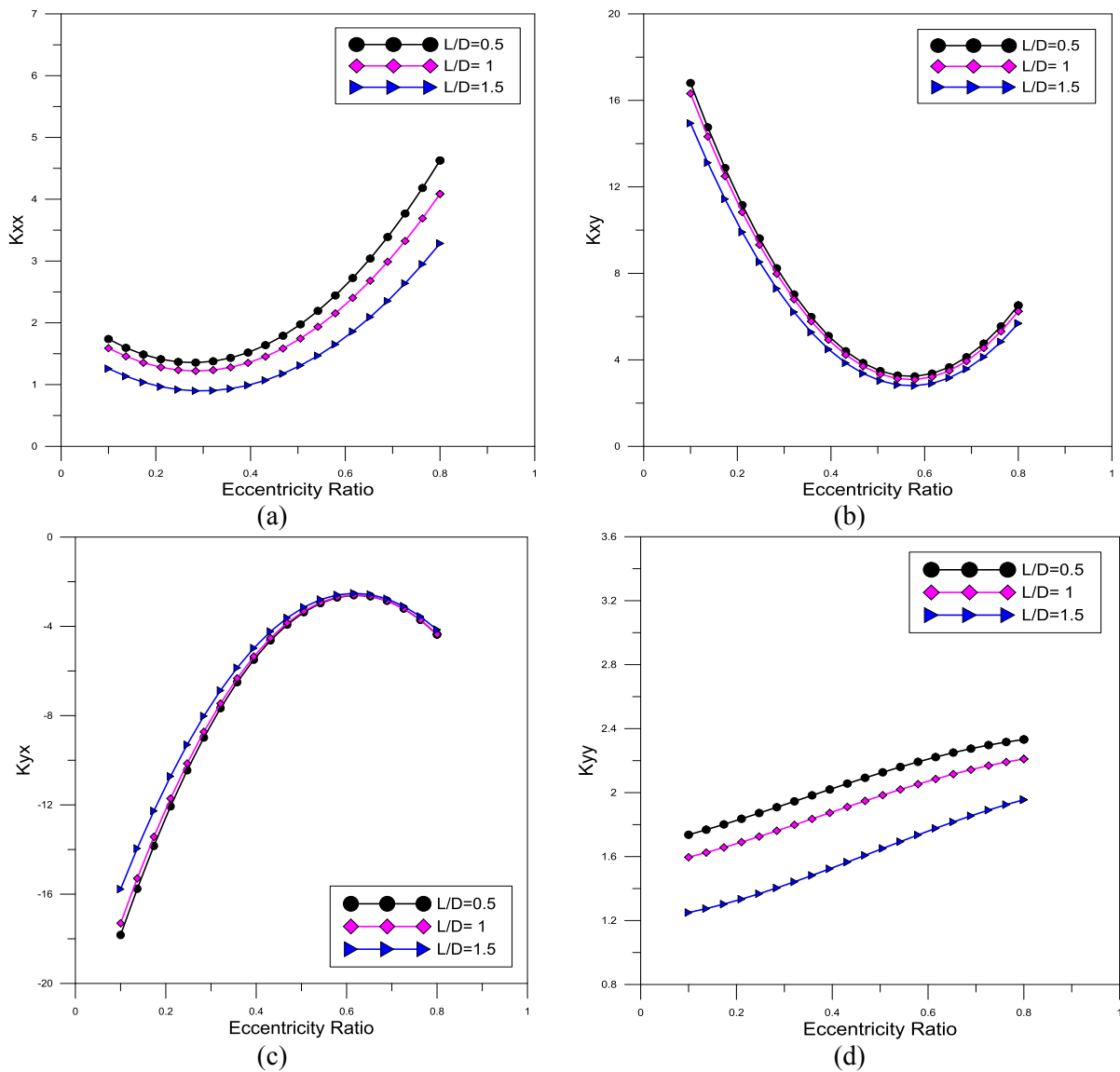


Figure 3. Dimensionless stiffness coefficients for different bearing length to diameter ratios.

The effects of bearing aspect ratios on the damping coefficients can be shown in Figures 4a to 4c. The effect of oil film temperature on these coefficients is also considered. It can be seen from Figure 4a that the damping coefficients (C_{xx}) always decrease when the bearing works at an eccentricity ratios in the range ($\varepsilon \leq 0.5$) after that it increases. This indicates that the force component in x-direction causes a higher journal center velocity as the bearing eccentricity ratio increases till 0.5. Also it can be seen from this figure that slight decrease in this dynamic coefficient has been obtained for the bearing that has higher aspect ratio. This can be imputed to the increase in oil film temperature in this case which causes a decrease in oil film viscosity. Figure 4b shows that the cross coupled damping coefficients ($C_{xy} = C_{yx}$) increasing when the bearing works at higher eccentricity ratios. This refers to the increase in bearing load component in x-direction when the bearing works at higher eccentricity ratio. This figure also shows that the bearing with higher aspect ratio has lower cross coupled damping coefficients. A 18% percentage decrease in C_{xy} has been calculated for a bearing that has an aspect ratio of 1.5 works at an eccentricity ratio of 0.6 in comparison with that has an aspect ratio of 0.5 works at the same eccentricity ratio. This can be attributed to the effect of oil film temperature on its viscosity. The direct damping ratio (C_{yy}) decreases for the bearing works at higher eccentricity ratios as can be shown from Figure 4c. A slight effect for the bearing aspect ratio on this coefficient has been noticed from this figure.

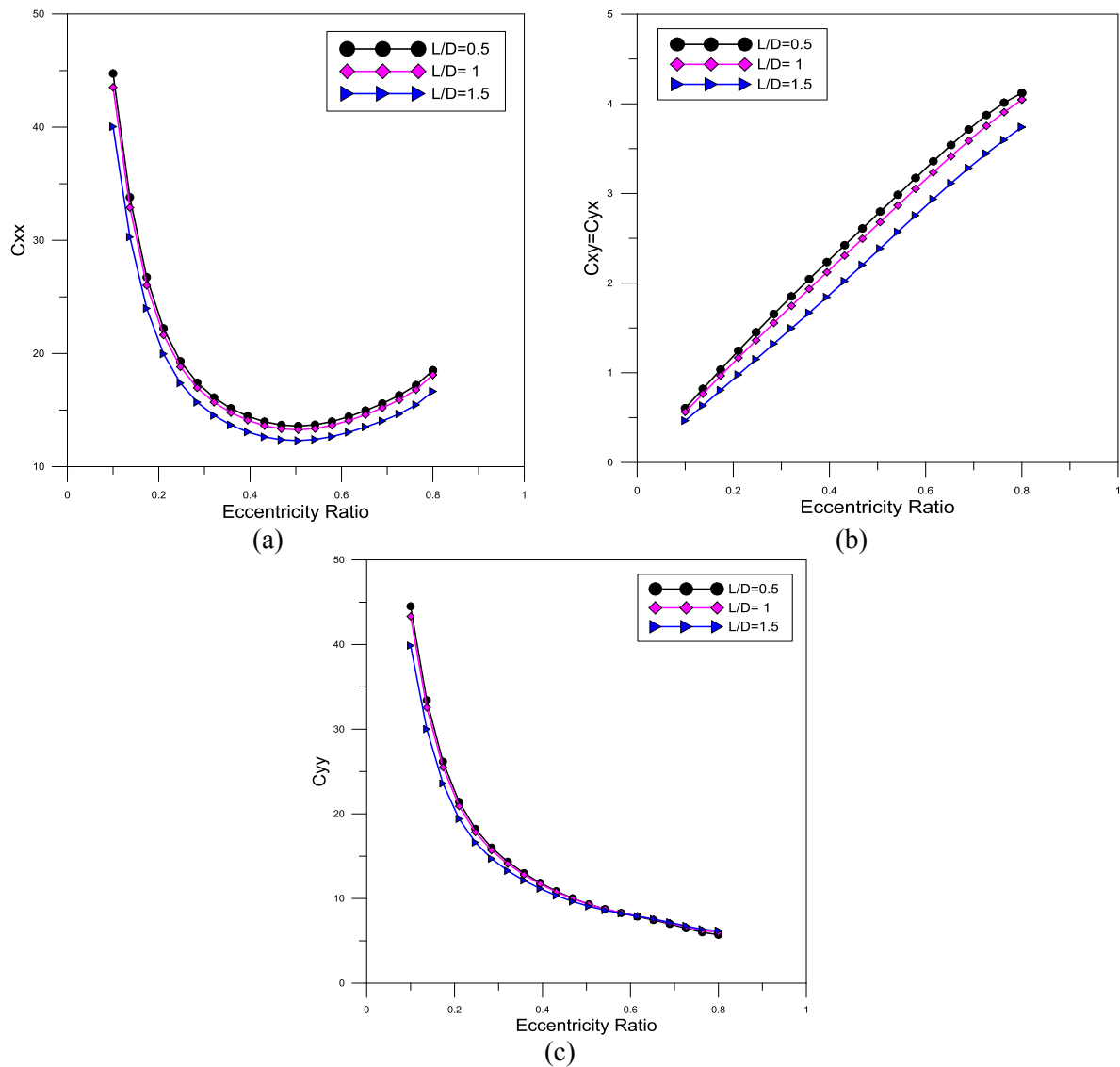


Figure 4. Dimensionless damping coefficients for different (L/D) ratios.

The dynamic stiffness and damping coefficients are used with the equations of motion to evaluate the stability of rotor bearing system. The effect of bearing length to diameter ratio on the parameters of stability such as the equivalent stiffness coefficient and critical mass can be shown from Figures 5 and 6. Figure 5 shows that the equivalent stiffness coefficient decreases with the increase of (L/D) ratios for the studied full range of eccentricity ratios. This can be imputed to the decrease of the direct stiffness coefficients of the oil film in this case which represent the main component of the equivalent stiffness. Figure 6 illustrates that the critical mass supported by the rotor generally increases when the bearing works at higher eccentricity ratios. A lower mass can be supported by the bearing that has higher aspect ratio. A percentage decrease in critical mass for a bearing works at eccentricity ratio of 0.6 was calculated and found to be 22% and 8.4% for a bearing has aspect ratios of 1.5 and 1 respectively in comparison with that have 0.5 aspect ratio. The percentage decrease of the critical mass becomes lower for the bearing works at higher eccentricity ratio.

Figures 7a to 7d shows the effect of the rotational speed on dimensionless stiffness coefficients. The dimensionless direct stiffness coefficient (K_{xx}) has been presented against the bearing eccentricity ratios as shown in Figure 7a. It is clear that the stiffness coefficient (K_{xx}) slightly decreases when the bearing works at lower eccentricity ratios (0.1 to 0.3), then the gaps between them grow thinner when the eccentricity ratio rising up. It is also clear from this figure that the stiffness coefficient increases as the journal speed increases. Increasing journal speed causes in a higher load component in x-direction and hence higher stiffness coefficient spatially when the bearing works at higher eccentricity ratio. The same behavior can be noticed for the direct stiffness coefficient K_{yy} as can be shown in Figure 7d.

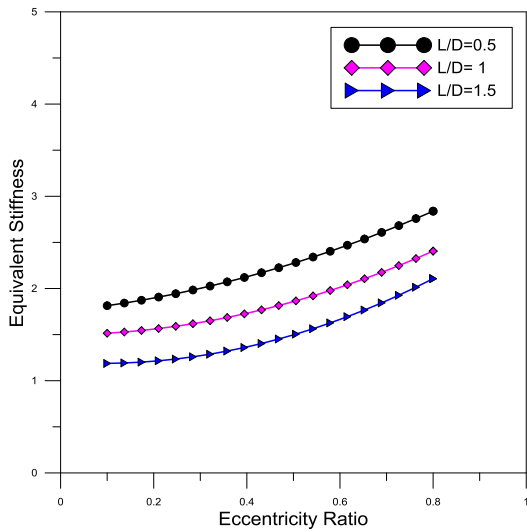


Figure 5. Equivalent stiffness.

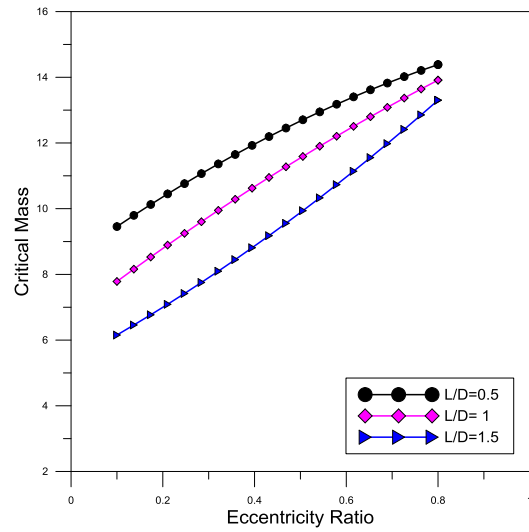
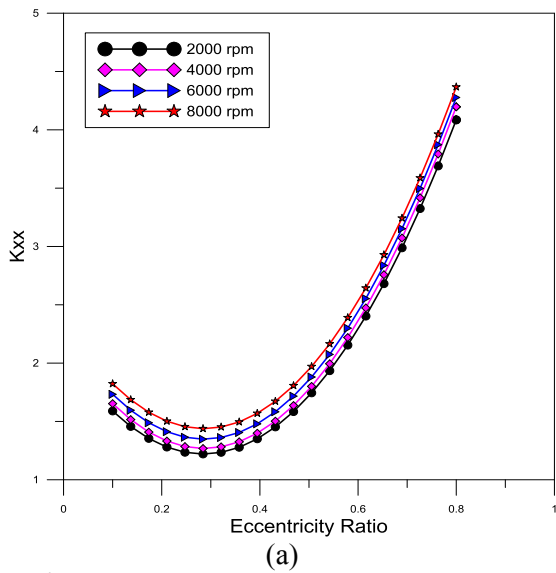
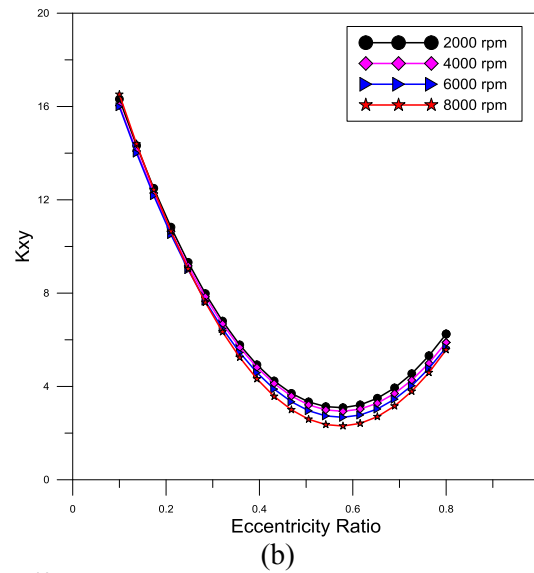


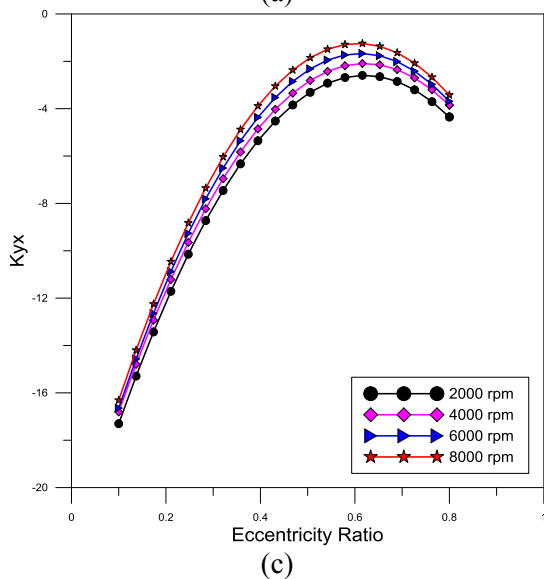
Figure 6. Critical mass.



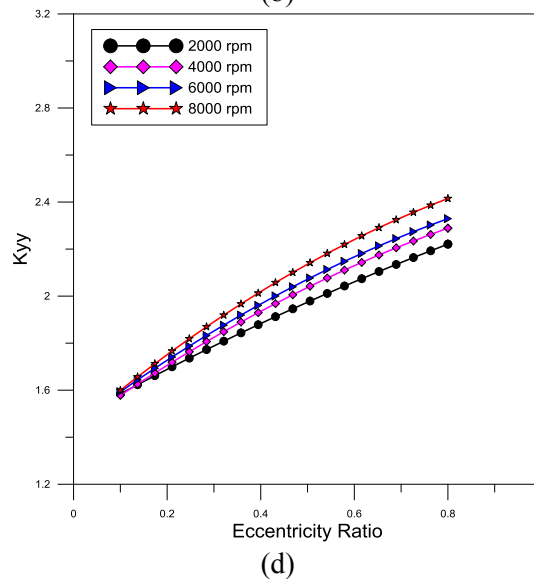
(a)



(b)



(c)



(d)

Figure 7. Dimensionless stiffness coefficients as a function of eccentricity ratios and different bearing rotational speed.

It can be observed from Figure 7b that the cross-coupled stiffness coefficient (K_{xy}) decreases when the eccentricity ratio less than 0.6, then stiffness coefficient (K_{xy}) takes an opposite behavior. Slight increase in K_{xy} as the journal speed increases has been noticed from this figure. The cross-coupled stiffness (K_{yx}) shows a negative values for all eccentricity ratio as can be shown from Figure 7c. This figure depicts that negative values of the (K_{yx}) slightly increases for the bearing works at eccentricity ratios less than 0.6 then decreases when the eccentricity ratio higher than 0.6. This figure also illustrates that the coefficient (K_{yx}) increases as the journal rotational speed increases.

The behavior of the dimensionless damping coefficients can be shown in Figures 8a to 8c for single grooved journal bearing considering the thermal effect against the eccentricity ratios for different rotational speed. The damping coefficients (C_{xx} , $C_{xy} = C_{yx}$ and C_{yy}) always increases when the rotational speed increases for all eccentricity ratios, the percentage of this increase is range about (22% to 36%) for rotational speed from 2000 rpm to 8000 rpm.

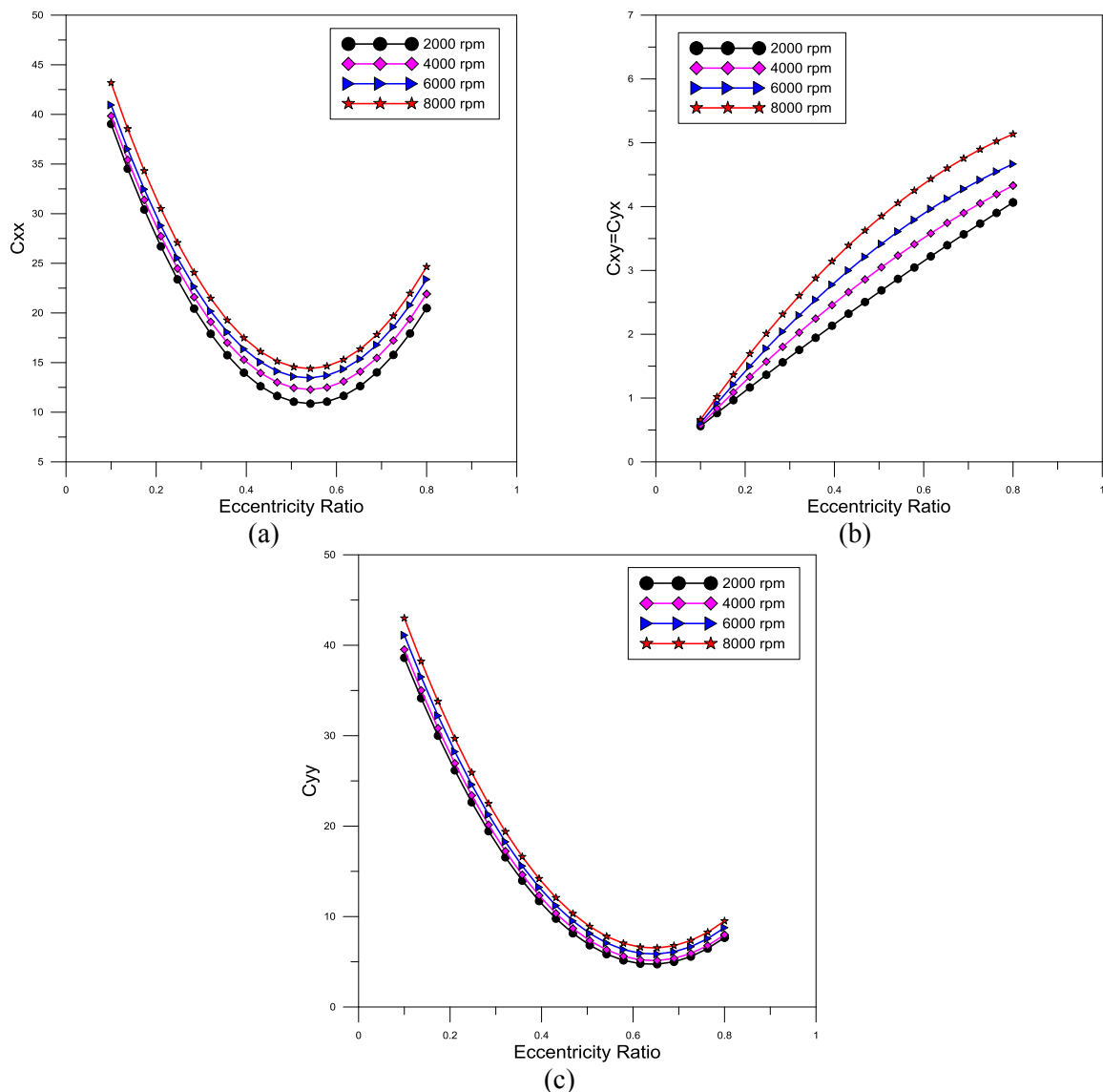


Figure 8. Dimensionless damping coefficients as a function of eccentricity ratios and different bearing rotational speed.

The effect of including oil film temperature on the calculation of equivalent stiffness and critical mass supported by the rotor can be shown in Figures 9 and 10. It is obvious from these figures that the equivalent stiffness and critical mass decrease when the temperature of the oil was considered. A percentage decrease of 33.3% in critical mass has been obtained when the bearing works at eccentricity ratio of 0.4 while it becomes 42% for the bearing with 0.5 eccentricity ratio. This can be attributed to the decrease in oil

viscosity due to the increase in oil film temperature which causes an increase in cross-coupled coefficients and decrease in direct dynamic coefficients and the equivalent stiffness. It can also be seen from these figures that the oil film temperature has a little effect on the stability of the bearing when it works at an eccentricity ratios less than 0.4.

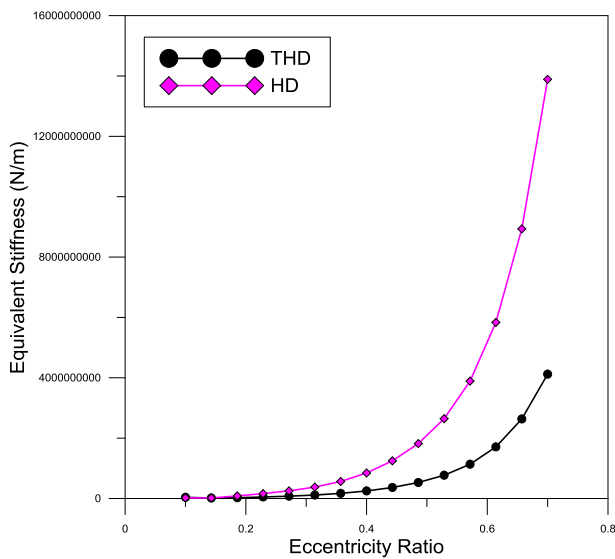


Figure 9. Dimensional Equivalent stiffness.

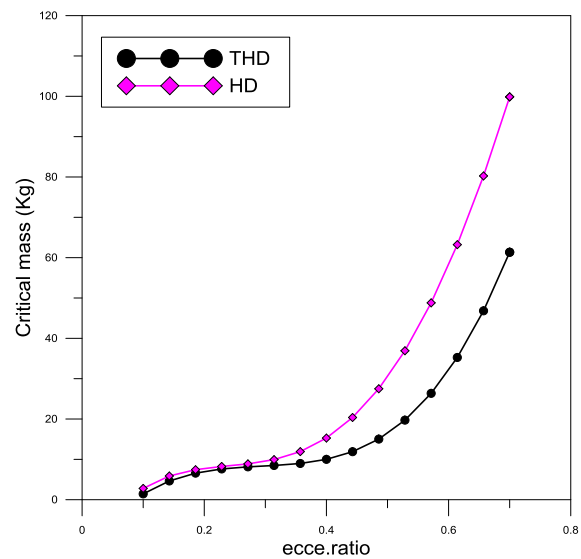


Figure 10. Dimensional critical mass.

8. Conclusion

The discussions of the obtained results lead to the following conclusion

1. The direct dynamic coefficients (stiffness and damping) decreased while the cross-coupled one increased when the oil film temperature was considered. This effect becomes more obvious for the bearing with higher aspect ratios.
2. Equivalent stiffness coefficient decreases for the bearing with higher aspect ratio. The decrease becomes higher when the oil film temperature was considered.
3. The critical mass supported by the rotor decreases for the bearing with higher aspect ratio.
4. The damping coefficients are generally increased for higher journal speeds.

The oil film temperature has a negative effect on the stability of the bearing. The critical mass decreases by 33.3 when the oil film temperature is considered for the bearing works at $\varepsilon = 0.4$.

Nomenclature

Symbol	Description	Units
c	Radial clearance	m
$D_{i,j}$	Damping Coefficient	$N \cdot s/m$
E	Complex number	-
F	Hydrodynamic Force	N
h, \bar{h}	Dimension and non-dimensional oil film thickness	m
$K_{i,j}$	Stiffness Coefficient	N/m
L	Bearing length	m
O_b, O_j	Bearing, journal centers	m
P	Oil film pressure	N/m^2
\bar{P}	Non-dimensional oil film pressure	-
R_s	Journal Radius	m
R_b	Bearing (bush) radius	m
R_{bi}	Bush inner radius	m
T, \bar{T}	Dimension and non-dimensional oil film temperature	$^{\circ}C$
T_o	Inlet temperature	$^{\circ}C$
U	Journal (shaft) speed	m / s
u, \bar{u}	Dimension and Dimensionless fluid velocity component in x-direction	m / s

v, \bar{v}	Dimension and Dimensionless Fluid velocity component in y-direction	m / s
w, \bar{w}	Dimension and dimensionless fluid velocity component in z-direction	m / s
<i>Greek symbols</i>		
β	Thermo-viscous coefficient	1/°C
ε	Eccentricity ratio	-
μ	Pure oil viscosity	Pa. s
μ_0	Inlet lubricant viscosity	Pa. s
θ	Angular coordinate	Deg.
φ	Attitude angle	Deg.
ω	Journal rotational speed	Rad/s

References

- [1] M. K. Lokhande and B.S. Prabhu, "Steady state and dynamic characteristics of partial journal bearings with variable viscosity effects"; Mechanism and Machine Theory, Vol.22, No.2, (1987).
- [2] R. Pai and B.C. Majumdar, "Stability of submerged oil journal bearings, considering thermal effects"; Wear, Vol.157 (1992).
- [3] R.S. Paranjpe, "A Study of Dynamically Loaded Engine Bearings using a Transient Thermohydrodynamic Analysis"; Tribology Transactions, Vol.39, (1996).
- [4] P. Michaud, D.Souchet, and D.Bonneau, "Thermo-hydrodynamic lubrication analysis for a dynamically loaded journal bearing"; Proceedings of the Institution of Mechanical Engineers, Vol.221, (2007) Part J: J. Engineering Tribology.
- [5] B.T.Paulsen, S.Morosiand I.F. Santos, "Static, Dynamic, and Thermal Properties of Compressible Fluid Film Journal Bearings"; Tribology Transactions"; Vol.54, No.2, (2011).
- [6] L.Gu and F. Chu, "An analytical study of rotor dynamics coupled with thermal effect for a continuous rotor shaft"; Journal of Sound and Vibration"; Vol.333 (2014).
- [7] D.S.Alves, G.B. Daniel and K.L. Cavalca, "Thermal Effects in Hydrodynamic Cylindrical Bearings"; Proceedings of the 9th IFToMM International Conference on Rotor Dynamics (2015).
- [8] F.Hemmati, M. Miraskari and M. S. Gadala, "Dynamic analysis of short and long journal bearings in laminar and turbulent regimes, application in critical shaft stiffness determination"; Applied Mathematical Modeling ; Vol.48 (2017).
- [9] S.Hamadavi, T.V.V.L.N Rao, M.Muhammad, K. M.Faez, "Liar stability analysis of short journal bearing with an axial groove" Mat.Wiss. u. Werkstofftech, 48,210-217, 2017.
- [10] L. Costa, A.S. Miranda, M.Fillon, J.C.P. Claro, "An analysis of the influence of oil supply conditions on the thermohydrodynamic performance of a single groove journal bearing"; Proceedings of the Institution of Mechanical Engineers ,Vol. 217,(2003), Part J: J. Engineering Tribology.
- [11] Boubendir S., Larbi S., Bennacer R., "A Contribution to the Analysis of the Thermo-hydrodynamic Lubrication of Porous Self-Lubricating Journal Bearings" Defect & Diffusion Forum Vol.297, (2010).
- [12] J. Ferron, J. Frene and R. Boncompain, "A Study of the Thermohydrodynamic Performance of a Plain Journal Bearing Comparison between Theory and Experiments" Journal of Lubrication Technology, Vol.105, No. 3, 422-428, (1983).
- [13] L. Roy, "Thermo-Hydrodynamic Performance of Grooved Oil Journal Bearing"; Tribology International, Vol.42, No. 8, 1187-1198, (2009).
- [14] W.Weimin, Y.Lihua, W.Tiejun and Y. Lie, "Nonlinear dynamic coefficients prediction of journal bearings using partial derivative method"; Proceedings of the Institution of Mechanical Engineers, Vol.226, No.4, (2012), Part J: Journal of Engineering Tribology.
- [15] L.Roy, and S. K. Kakoty, "Optimum groove location of hydrodynamic journal bearing using genetic algorithm"; Advances in Tribology, Volume 2013, Article ID 580367, 13 pages <http://dx.doi.org/10.1155/2013/580367>.
- [16] Basim A. Abass and Muhamed A. Munier, "Static and Dynamic Behavior of a Rotor Supported on TiO2 Nano Lubricated Journal Bearings"; Accepted for publication in Association of Arab Universities Journal of Engineering Science (2017).
- [17] Qiu,Zhi Ling "A Theoretical and Experimental Study on Characteristics of Journal Bearings"; Doctor of philosophy thesis, Dept. of Mechanical Engineering, University of Wollongong, (1995).
- [18] D. Sheeja and B. S. Prabhu, "Thermal and Non-Newtonian Effects on the Steady State and Dynamic characteristics of Hydrodynamic Journal Bearings-Theory and Experiments"; Tribology Transactions, Vol. 35, (1992).